

Energy Advances

Accepted Manuscript

This article can be cited before page numbers have been issued, to do this please use: A. Mostafa, A. Beretta, G. Groppi, E. Tronconi and M. C. Romano, *Energy Adv.*, 2025, DOI: 10.1039/D4YA00540F.



This is an Accepted Manuscript, which has been through the Royal Society of Chemistry peer review process and has been accepted for publication.

Accepted Manuscripts are published online shortly after acceptance, before technical editing, formatting and proof reading. Using this free service, authors can make their results available to the community, in citable form, before we publish the edited article. We will replace this Accepted Manuscript with the edited and formatted Advance Article as soon as it is available.

You can find more information about Accepted Manuscripts in the [Information for Authors](#).

Please note that technical editing may introduce minor changes to the text and/or graphics, which may alter content. The journal's standard [Terms & Conditions](#) and the [Ethical guidelines](#) still apply. In no event shall the Royal Society of Chemistry be held responsible for any errors or omissions in this Accepted Manuscript or any consequences arising from the use of any information it contains.

Novel Electrified Sorption Enhanced Reforming Process for Blue Hydrogen Production

Abdelrahman Mostafa^{1*}, Alessandra Beretta¹, Gianpiero Groppi¹, Enrico Tronconi¹, Matteo C. Romano^{2*}

¹ LCCP – Laboratory of Catalysis and Catalytic Processes, Dipartimento di Energia, Politecnico di Milano, Via la Masa 34, 20156, Milano, Italy.

² GECOS – Group of Energy Conversion Systems, Dipartimento di Energia, Politecnico di Milano, Via Lambruschini 4, 20156, Milano, Italy.

*Corresponding authors: abdelrahmanmohamed.mostafa@polimi.it, matteo.romano@polimi.it

Abstract:

Sorption Enhanced Reforming (SER) emerges as a promising solution for the deployment of blue hydrogen and offers the flexibility to accommodate future green feedstocks. This study assesses the techno-economic feasibility of implementing electrified reactors for the endothermic sorbent regeneration step in SER-based hydrogen production plants, introducing the novel electrified sorption enhanced reforming (eSER) process. The analysis is conducted by integrating a 1-D dynamic heterogeneous model of an adiabatic fixed bed reactor into a process model of the complete plant. A natural gas-based hydrogen production plant with 30000 Nm³/h capacity is considered, simulating five different cases, two of which with advanced plant configurations designed to capture more than 90% of the feed carbon. Evaluating a set of key performance indicators that covers technical, environmental, and economic aspects of the process, these simulated cases are benchmarked against existing studies utilizing conventional and state of the art steam methane reforming with carbon capture technology from literature. The findings highlight the remarkable performance of eSER, achieving specific electric consumption of 12-14 kWh/kg_{H₂} and natural gas to H₂ conversion efficiency exceeding 100% calculated on chemical energy basis. For the base case configuration an overall energy efficiency of eSER process of 74.3% and a CO₂ capture rate of 86.3% are computed. For the advanced configurations, energy efficiency of 73.7% and 73.1%, CO₂ capture rates of 90.3 and 96.6% and levelized cost of hydrogen of 2.50 and 2.52 €/kg_{H₂} have been obtained.



Keywords: Electrified reactors; CO₂ capture; Hydrogen; sorption enhanced reforming; Process Modeling; Economic analysis.

1. Introduction:

Hydrogen can play a crucial role in reducing the carbon footprint of hard-to-decarbonize industries and for long duration energy storage. Additionally, it holds great importance as a chemical product, finding extensive use in refinery applications and serving as a fundamental platform in the production of key chemicals such as ammonia and methanol ¹.

Currently, hydrogen production is largely dependent on the unabated use of fossil fuels, with natural gas contributing to 62% of global production, primarily through the steam methane reforming process (SMR) ². In conventional SMR plants, fossil fuel combustion generates heat to drive the strongly endothermic steam methane reforming reaction, leading to the emission of substantial amounts of CO₂-containing flue gas; a typical fired SMR process using natural gas emits around 10 kg CO₂/kg H₂ ³. In such hydrogen production plant, two main sources of CO₂ emissions exist: i) CO₂ resulting from the methane reforming reaction (syngas CO₂), with a molar percent approaching 15%mol on dry basis, and ii) CO₂ resulting from combustion of fossil fuels to provide the necessary heat for the process, with a molar percentage of about 4% mol on dry basis. While technology to separate CO₂ from syngas has been available commercially for decades for ammonia production, the highly diluted CO₂ in the combustion effluents makes the downstream carbon capture process more challenging ⁴.

Given that the steam methane reforming process has been the dominating technology for hydrogen production, setting the reference hydrogen price in the market, several research activities have focused on improving the efficiency of the SMR process addressing different aspects of a typical H₂ production plant ⁵. Among the technologies extensively studied, the sorption enhanced reforming has re-emerged as a promising candidate for blue hydrogen production ⁶. Sorption enhanced reforming is a two-step process where initially, hydrocarbons reforming takes place in the presence of reforming catalyst and CO₂ sorbent. The presence of the CO₂ acceptor in the catalytic reactor results in the removal of the CO₂ from the reaction zone, shifting the thermodynamic equilibrium towards higher CH₄ and CO conversion ⁷. An additional advantage is the substantial heat evolution resulting from the exothermic reaction between CO₂ and the solid sorbent



eliminating the need of external heat addition for reforming^{8,9}. Upon the saturation of the sorbent, a subsequent highly endothermic step of sorbent regeneration is required.

The nature of the SER process, alternating between the two steps of reforming and regeneration, makes it an ideal candidate to be conducted in interconnected fluidized bed reactors, where the bed fluidization ensures homogeneous sorbent properties and low temperature gradients in the reactors both in the reforming and regeneration steps¹⁰. Several studies have been performed to evaluate the SER process of full-scale hydrogen production plants. The technology has been validated through experimental studies and is currently classified at Technology Readiness Level (TRL) 4¹¹. Recently, pilot plant experimental studies were initiated to advance the technology to the next TRL. Among these, the Gas Technology Institute (GTI) conducted a pilot-scale study, producing approximately 71 kW_{th} of hydrogen with a purity exceeding 80%¹². In order to achieve a feasible CO₂ abatement, the regeneration step must be conducted in a manner that results in concentrated streams of CO₂. Thus, the conventional use of hot flue gases arising from fuel combustion in air as direct medium for the sorbent regeneration is not possible for this application. A first option is to perform sorbent regeneration by oxyfuel combustion of natural gas and PSA off-gases. The integration of an oxyfuel SER process in a hydrogen production plant was assessed by Martínez et al.¹³, who proposed plant designs achieving 74.2-76.6% equivalent hydrogen production efficiency and over 98% carbon capture ratio. More recently, as an alternative sorbent regeneration option, many studies addressed the integration of the SER process with the chemical looping technology, avoiding the need for an air separation unit. Zhu and Fan¹⁴, Alam et al.¹⁵, and Phluanglue et al.¹⁶ have studied combining Ni-NiO chemical cycle with the SER process to provide the heat required for the sorbent regeneration. An additional air reactor is used to realize the exothermic Ni oxidation, resulting in heating up of the Ni based pellets that are then recycled to the fuel reactor where the reduction of NiO occurs with CH₄. The heat released from the Ni-NiO cycle covers the heat demand for the sorbent regeneration in the calciner. Results presented in¹⁵, shows that the process can achieve a hydrogen production efficiency of 70.7% while capturing 95.1% of the feed carbon. Yan et al.⁶ have evaluated the competitiveness of different SER configurations for blue H₂ production. In their work, H₂ production by SER-based processes equipped with: i) calciners externally heated; ii) chemical looping combustion (CLC); or iii) H₂ fired calciners were assessed. The authors showed that combining the SER with CLC could achieve a theoretical hydrogen production efficiency (Cold gas efficiency) of 75.5% while capturing almost



100% of the carbon fed to the plant. H₂-fired calciner presents the worst theoretical performance, where an efficiency of around 51% and a carbon capture ratio of 94.2% were calculated. In comparison, internally heated oxy-fired calciner results in a hydrogen production efficiency of 72.8% and a CO₂ capture ratio approaching 100%.

A drawback of fluidized bed-based SER processes is related to the need to operate the interconnected fluidized bed system at low pressure difference between the reactors. Thus one of two solutions must be implemented for the calciner: (i) a process operating at high pressure (20 - 40 bar) but at calcination temperature far above 1000°C, (ii) a process operating at lower pressure and temperature which in turn requires challenging equipment to move the sorbent between the reformer and the calciner¹⁷. On the other hand, fixed bed SER systems can be operated with pressure swing between the reforming stage, to be operated at high pressure, and the sorbent regeneration stage, to be operated at low pressure to avoid exceeding the catalyst and sorbent temperature limits. To overcome the technical challenges of high temperature heat transfer from hot combustion products in fixed bed SER reactors, novel approaches are required such as the integration of a Cu-CuO chemical looping cycle. The Ca-Cu process concept was originally proposed by¹⁸ and then underwent several experimental and modelling developments¹⁹. Riva et al.²⁰ studied the integration of the Ca-Cu process in a full-scale hydrogen plant, estimating a hydrogen production efficiency of 74.1% with a carbon capture ratio of 95.6% and a levelized cost of hydrogen of around 2.1 €/kg_{H₂}.

Even though sorption enhanced reforming is one of the very promising technologies for hydrogen production, the limitations that currently the process faces hinders its large scale implementation. Key challenges include the degradation and instability of sorbents during repeated cycles²¹, high energy demands for sorbent regeneration, and CO₂ slip²². The integration of reforming and CO₂ capture in a single reactor increases process complexity, making scale-up and control more challenging. These limitations underscore the need for advancements in sorbent materials, reactor design, and renewable energy integration to enhance the process's sustainability and scalability.

Recently, Tronconi et al.²³ proposed the use of thermally conductive metallic and ceramic internals for mitigating the intrinsic heat transfer limitations of non-adiabatic processes. The study was extended later on presenting the packed foam reactor configuration where the empty porosity of open cell metallic foams was filled with active particles resulting in high reactor inventory of the



active phase ²⁴. These enabling features, that is the presence of conductive internals that can be packed with catalyst and sorbent particles, offer a solution to alleviate heat transfer limitations in fixed bed SER systems, avoiding high temperature heat transfer surfaces and preserving the properties of catalyst and sorbent.

Besides, given the substantial increase of the share of renewable energy sources transforming the electric energy production sector, the exploitation of electric energy as an unconventional method to provide heat for chemical reactions has been recently proposed ²⁵. Works in the literature have confirmed the suitability of different heating approaches, including induction heating ²⁶⁻²⁸, microwave heating ²⁹, and resistive ohmic heating ^{3,30-33}, for overcoming the heat transfer limitation in heterogenous catalytic systems. The inherent characteristic of the aforementioned heating systems of delivering the required heat locally has resulted in homogenous temperature profiles across the reactors, proving the technical possibility of uniform heat delivery. Compared to induction heating and microwave heating, resistive ohmic heating is expected to have a higher thermal efficiency as a result of the direct conversion of electric energy into thermal energy ³². Additionally, resistive ohmic heating is a commercially available technology, thus, rapid integration in novel processes is feasible.

In this context, this study proposes implementing electrified reactors with conductive internals for the endothermic sorbent regeneration step of a SER-based H₂ production plant, giving rise to the novel process of Electrified Sorption Enhanced Reforming (eSER), herein proposed. The process leverages the use of resistive ohmic heating, in the presence of the thermally conductive internals, as a solution for the key technological hurdle of the process (i.e. the sorbent regeneration step) ensuring homogeneous heat delivery for sorbent regeneration. The analysis evaluates the techno-economic feasibility of the concept relying on a previously developed 1-D dynamic heterogeneous model of a fixed bed reactor to predict the reactor's behavior ³⁴. The proposed process includes, besides the eSER reactors network, stages for H₂ and CO₂ separation and compression. The process is modeled using ASPEN plus software and the analysis compares key performance indicators (KPIs) calculated for the electrified SER plant (eSER) with conventional SMR fired tubular reformer (FTR) and electrified SMR plants including carbon capture units.



2. Process concept

A typical industrial hydrogen production plant consists of a series of units namely: a desulphurization section, a pre-reformer, the primary reformer, water gas shift (WGS) reactors, and H₂ purification by pressure swing adsorption (PSA). In case of CO₂ capture, the plant is also equipped with a CO₂ separation section, either from: i) syngas, ii) PSA off-gas, or iii) SMR furnace flue gas. Due to the nature of the sorption enhanced reforming process, where reforming, WGS, and CO₂ removal are combined in the same reactor, the proposed eSER process provides a simplified plant scheme. An ideal arrangement of the eSER process can approach a continuous steady production of hydrogen through alternating parallel reactors between the two steps of the process: the sorption enhanced reforming and the sorbent regeneration passing through the two intermediate steps of blow down and re-pressurization as presented in **Figure 1**. In the reforming step, the fuel and steam react in the presence of the active sorbent resulting in the production of a concentrated stream of Hydrogen. Ideally the reforming step can be designed to work adiabatically, without the need of heat addition, where the demand of the endothermic SMR is provided by the CO₂ sorption reaction and the bed thermal capacity. Subsequently to the reforming step, the reactor is depressurized, then it is switched to the regeneration step configuration where the solids are heated electrically, and the captured CO₂ is released. Finally, the reactor is repressurized up to the reforming pressure and the cyclic process starts again.



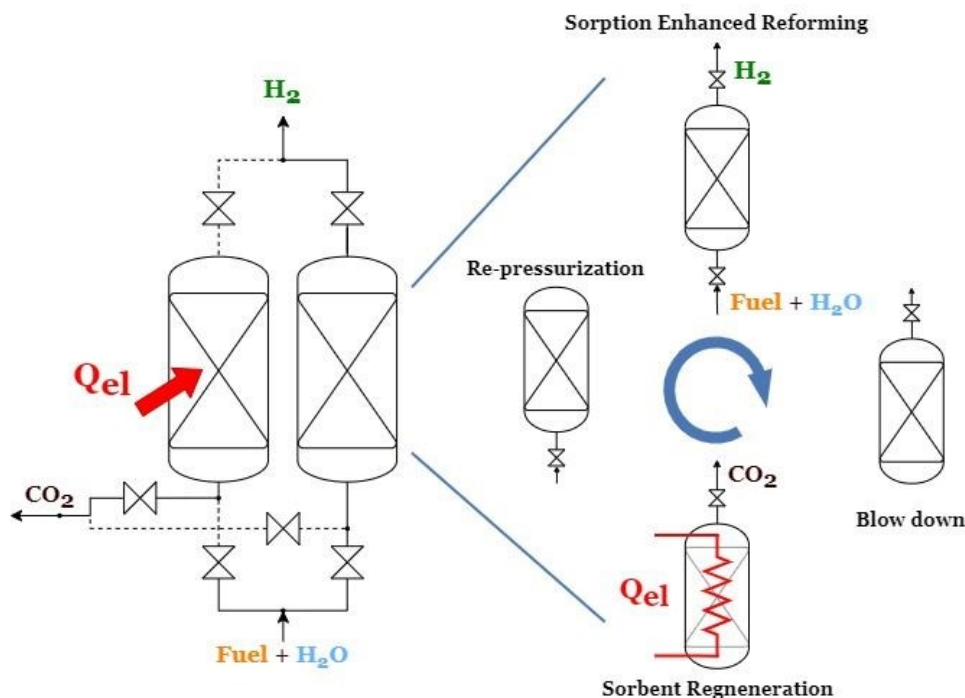


Figure 1 Electrified Sorption Enhanced Reforming concept (eSER)

In order to obtain a stream of hydrogen with high purity, exceeding 99%, a conventional PSA unit is needed downstream the eSER reactors network. The low-pressure PSA off-gas stream, characterized by its low carbon content, is combusted to generate steam and preheat the feed. The proposed process block diagram is presented in **Figure 2**.

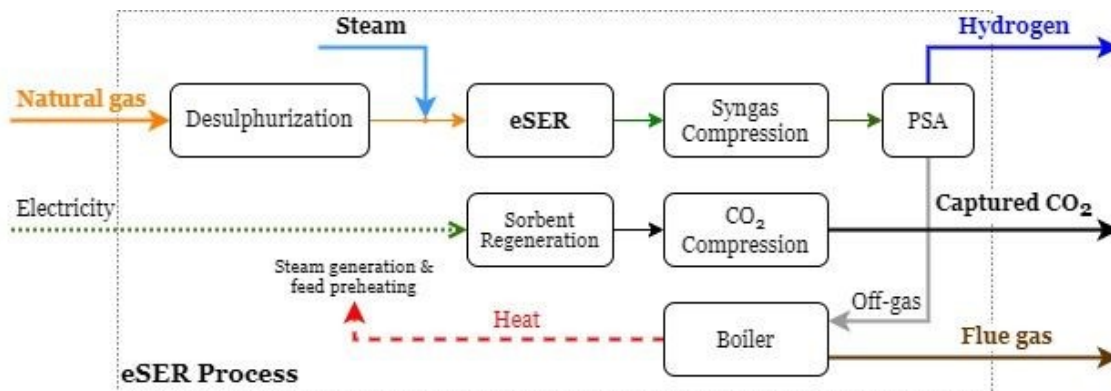


Figure 2 eSER process block diagram



3. Methods

As presented in **Figure 1**, a typical eSER reactor passes by four main steps: Sorption Enhanced Reforming, Blow down, Sorbent Regeneration, and Re-pressurization. Given that depressurization and re-pressurization steps are very short and have a negligible effect on the process, only the reforming and regeneration steps can be considered for modeling purposes. Regarding the full-scale process, where multiple reactors are operating in parallel with time mismatch to produce a steady flow of hydrogen, quasi steady state can be considered for the flow exiting the reactors. Thus, the eSER based hydrogen production plant is modeled to work under steady state conditions using AspenPlus® process simulation software. The adopted modeling approach has been used in many studies present in the literature based on high temperature packed bed systems both for sorption enhanced reforming and chemical looping processes^{19,20,35–42}.

3.1. 1D SER reactor modeling

Starting with the reforming step of the process, being the most complex step where different reactions occur and where the reactor productivity is determined, the reactor behavior during the reforming step is modeled using a 1D reactor model. In a previous work³⁴, a heterogeneous one-dimensional dynamic model of methane sorption enhanced reforming in an adiabatic fixed bed reactor has been developed. The model describes the dynamic evolution of concentration and temperature axial profiles across the SER reactor by solving the dynamic differential mass and energy balances and incorporating the kinetics and thermodynamics of all chemical processes. The model was further extended to include the presence of C2+ hydrocarbons in the feed⁴³ making it suitable for a typical natural gas stream. The model is implemented in gPROMS® software platform for dynamic simulation following the numerical scheme detailed in our previous work³⁴. Noteworthy, the electric components needed for heating the reactor during the regeneration step of the process are modeled as inert solids. The addition of this inert phase is important to consider the role of the thermal capacity of the reactor on the eSER process, both in the reforming and the regeneration steps.

As explained by Riva et al.²⁰, dividing the required reactor volume into several sub-reactors sharing the same set of valves allows for a reduced vessel cost sustaining a proper length to diameter ratio. The same approach is used in this study, where six sub-reactors with a diameter of



2.25m and a length of 5m are assumed to collectively form the total reactor volume required for the production of 30000 Nm³/h of hydrogen. Each sub-reactor is modeled using the 1D reactor model and the time-average yields of all the species are computed by integrating the temporal flow profiles of the species entering and exiting the sub-reactor and ratioing them to the time on stream. Accordingly, for the full-scale process analysis, the collective eSER sub-reactors are modeled as a series of elementary units that reproduce the heat and mass balances of the reforming step of the process. The sub-reactor characteristics and the assumptions used in the 1D reactor model simulations are reported in Section A of the Supplementary Material.

3.2. Full-scale process modeling

As discussed in section 2, the eSER hydrogen production plant would ideally contain two or more reactors, each operating in one of the steps of the process to guarantee the continuous production of hydrogen. As presented in **Figure 3**, the simplified scheme of the modeled eSER H₂ production plant can be divided into four main units: natural gas pretreatment unit, eSER reactors (operating both in SER and regeneration), hydrogen compression and purification unit, CO₂ compression and liquification section. Additionally, the PSA-off gas leaving the H₂ purification unit is combusted to provide the heat required to balance the plant, representing the source of emissions in the plant.

In the core of the process the SER reactors, modeled as bundle of sub-reactors, assume an input-output model reproducing the time-average yields of all the species as calculated by the 1D reactor model. A set of reactors, mixers, separators, and heaters are used to reproduce the mass and energy balances of the process as computed by the 1D reactor model. The methodology used for modelling is detailed in Section A of the supplementary material. This approach results in closing the material and enthalpy balances with a minor difference compared with the results of the 1D dynamic reactor model (<1% for the total mass and enthalpy balances). The differences in the balances are resulting from numerical errors in the 1D reactor model that led to higher errors in the overall mass and energy balance over a SER cycle. Typical values of the calculated variations in the material and enthalpy flows comparing the steady state ASPEN model and the 1D dynamic heterogeneous reactor model are reported in Table A2 in Section A of the supplementary material.



in the reactor eliminates the presence of sharp thermal gradients during the regeneration step. Similar behaviour was shown experimentally by Balzarotti et al.⁴⁵ and Zheng et al.⁴⁶ for heat delivery to highly endothermic reactions.

It is worth mentioning that due to the dynamic nature of the process, the streams leaving the SER reactors, both in reforming and regeneration steps, are expected to exhibit variable temperatures and flow rates. To limit thermal fatigue issues for the heat exchangers and instabilities of the reactor feed stream properties, indirect heat recovery is proposed, where the effluents of the reactors are used to generate saturated steam at different pressures that, while acting as a buffer, is later on used for preheating and evaporation of the main process steam. The main process assumptions are reported in **Table 1**.

Table 1 Main process assumptions for the simulations of the eSER H₂ production plant

Natural gas (NG)		
Composition	CH ₄ :89; C ₂ H ₆ :7; C ₃ H ₈ :1; CO ₂ :2; N ₂ :1	vol %
LHV		46.9 MJ/kg
NG supply temperature		25 °C
NG pre-treatment		
Operating temperature of the desulfurization unit		365 °C
Pressure loss in the desulfurization unit		0.3 bar
eSER process		
Reforming step		
Feed temperature		550 °C
Steam to carbon ratio		4 - 6*
Operating pressure		10 - 30* bar
Regeneration step		
Regeneration temperature		900 - 800* °C
Regeneration pressure		1 - 0.2* bar
Heat recovery		
ΔT_{\min} gas-gas heat exchangers		20 °C
ΔT_{\min} gas-evaporating water heat exchanger		10 °C
Evaporation pressure		10 - 30 bar
T _{in} water		15 °C
T _{out} cooling water		25 °C



Intercooled compressors

Isentropic efficiency	72 %
Electromechanical efficiency	94 %
Intercool water temperature	35 °C

Pumps

Hydraulic efficiency	70 %
Electromechanical efficiency	94 %

Hydrogen purification unit

PSA feed pressure	30 bar
Pressure loss in the PSA unit	1 bar
Hydrogen recovery efficiency	90 %

Combustors

Air composition	N ₂ : 79; O ₂ : 21 vol %
T _{in} air	20 °C
Hydrogen delivery pressure	29 bar
Liquified CO ₂ delivery pressure	110 bar

*Values depend on the modeled case

The analysis is performed for a medium scale H₂ production plant with a productivity of 30000 Nm³/h. This study covers five cases, three of which are unconstrained by preset KPIs and are intended to examine the eSER performance under different configurations, while the remaining two aim for a carbon capture ratio (CCR) exceeding 90%. Maximizing the CCR is of the utmost importance to align with the current guidelines set by the European Union for low carbon hydrogen set since January 2021 at 3.38 kg_{CO2}/kg_{H2} by the renewable energy directive EU 2018/2001 (RED II). The unconstrained cases assess the impact of specific working conditions - namely, the reforming pressure and the regeneration pressure- on the technical and economic performance indices of the plant.

An increase in the reforming pressure of the plant is predicted to reduce the capital expenditure (CAPEX), as it eliminates the need for an expensive gas compressor to deliver the impure hydrogen to the PSA unit at the design pressure of 30 bar. However, a higher reforming pressure is projected to result in lower methane conversion, leading to reduced hydrogen production. Besides, lowering the regeneration pressure implies a reduced regeneration temperature, which in turn lowers the heating demand of the plant, predicting a decrease in the plant operating costs. It is important to



note that delivering the CO₂ at lower pressure necessitates higher compression power for delivering the liquified CO₂ at the specified pressure of 110 bar.

As the sorption-enhanced reforming process integrates the functionalities of a steam reformer, shift reactor, and CO₂ removal into a single reactor, a high steam-to-carbon ratio is needed to increase hydrocarbons conversion and carbon capture, as demonstrated in the literature^{34,43,47}. In the unconstrained simulated cases (base case, high-pressure reforming, and vacuum regeneration), the selected steam-to-carbon ratio is determined by the maximum amount of steam producible through heat recovery in the plant.

To increase the CO₂ capture efficiency above 90%, two cases have been considered:

- low-pressure steam generation and steam compression (**Figure 4**): this configuration allows to increase steam production by improved heat recovery, while the steam compressor raises the steam pressure to the reforming pressure of 10 bar.
- Three-stage eSER-eSMR-eSEWGS process (**Figure 5**): in this configuration the eSER reactor is designed to work at high pressure, leading to moderate methane conversion. To increase CH₄ conversion and CO₂ capture, the effluent of the eSER reactor is first delivered to an electrified steam methane reformer (eSMR) operating at 950°C that achieves high methane conversion. At the outlet of the eSMR reactor, an electrified sorption enhanced water gas shift (eSEWGS) step is added, converting CO while capturing CO₂ on CaO-based sorbent at high temperature. The adoption of the eSEWGS step is necessary to improve the carbon capture performance given that there are no downstream CO₂ capture units in the typical eSER process scheme. Thus, this configuration improves carbon capture efficiency by decoupling the SMR from CO₂ sorption reactions to capture the last portions of the carbon dioxide.



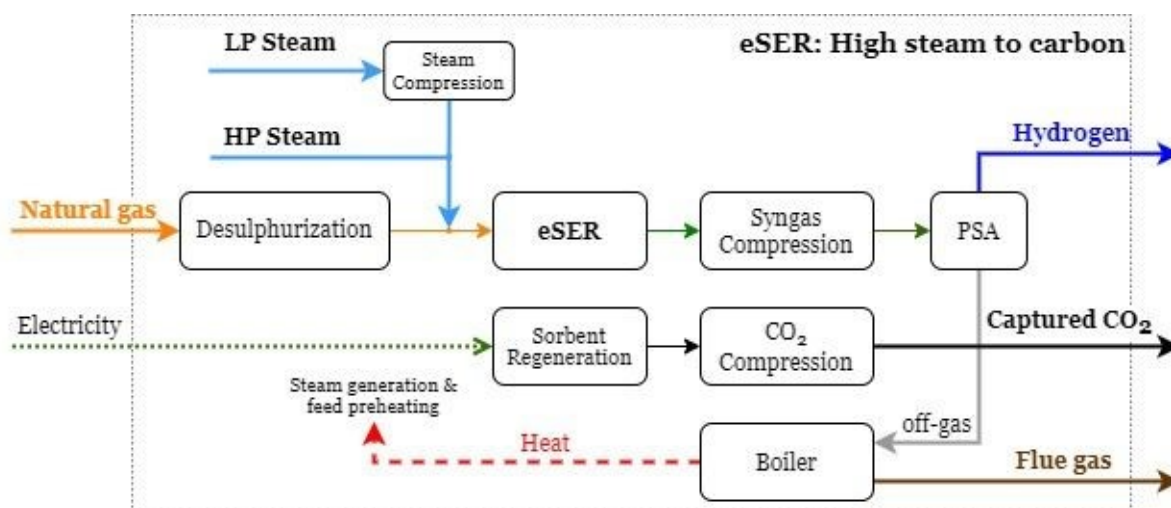


Figure 4 eSER with high steam to carbon case block diagram

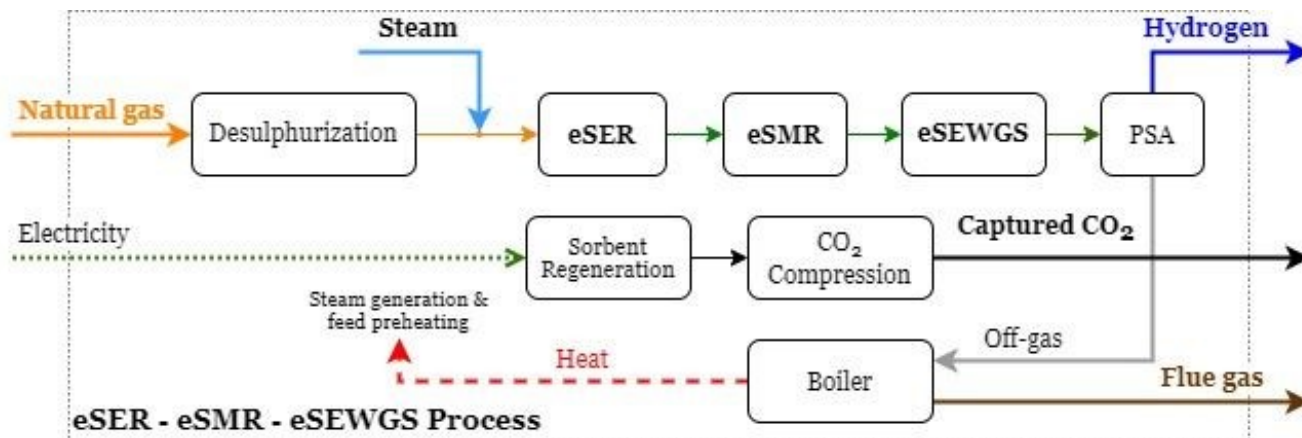


Figure 5 eSER - eSMR - eSEWGS process block diagram

3.3. Key performance indicators

The technical performance of the different plant arrangements is evaluated based on a series of key performance indicators. Noteworthy, the same definitions of the performance indicators have been used to evaluate other similar processes allowing for the direct comparison of the novel eSER process with hydrogen production processes found in the literature ⁴⁸.

As commonly used in the literature, the H₂ production efficiency (η_{H_2}) is defined as the ratio between the chemical energy flow rate of the produced hydrogen and the input chemical energy flow rate of the natural gas as defined in Eq. 1.

$$\eta_{H_2} = \frac{\dot{m}_{H_2} LHV_{H_2}}{\dot{m}_{NG} LHV_{NG}} \quad \text{Eq. 1}$$



The total efficiency (η_{tot}) of the plant is calculated, as presented in Eq. 2, to include the input electric power consumed within the plant battery limit.

$$\eta_{tot} = \frac{\dot{m}_{H_2} LHV_{H_2}}{\dot{m}_{NG} LHV_{NG} + P_{el}} \quad \text{Eq. 2}$$

Carbon capture ratio (CCR), Eq. 3, is computed as the molar flow of the captured CO₂ divided by the total molar flow of carbon entering the plant as natural gas.

$$CCR = \frac{\dot{n}_{CO_2 \text{ captured}}}{\dot{n}_{C-NG}} \quad \text{Eq. 3}$$

Given that the eSER is a net importer of electricity, an indicator referring to the equivalent CO₂ (CO_{2,eq}) is necessary to account for the indirect CO₂ emission associated with electricity consumption. Equivalent CO₂ emissions (E_{CO_{2,eq}}) as presented in Eq. 4, considers both the process direct emissions, such as combustion flue gas, and indirect emissions rising from importing electricity from the grid, and from GHG emissions alongside the natural gas supply chain (Methane leakage and emissions related to production and transportation of NG). E_{CO_{2,eq}} is defined in Eq. 4, where ($\dot{m}_{CO_2 \text{ emitted}}$) is the direct emissions from the plant, CI_{grid} is the grid carbon intensity in the geographical location of the H₂ production plant, LR_{CH₄} is the equivalent methane leakage rate, which includes the GHG emissions rising from the NG supply chain, and GWP_{CH₄} is the global warming potential of methane.

$$E_{CO_2,eq} = \frac{\dot{m}_{CO_2 \text{ emitted}} + P_{el} CI_{grid} + \dot{m}_{NG} LR_{CH_4} GWP_{CH_4}}{\dot{m}_{H_2}} \quad \text{Eq. 4}$$

3.4. Economic Modeling

The economic analysis is performed following a “bottom-up” approach where, initially, the capital costs of each installed equipment are estimated by means of cost functions as reported in ⁴⁹. Notably, all the calculated costs are referenced to the same year, 2022, using the Chemical Engineering Plant Cost Index (CEPCI), estimated at 709. The variables used for the equipment cost function parameters, along with the corresponding reference CEPCI, are tabulated in Section A of the supplementary material.

Regarding the novel eSER reactor cost estimation, the simplified reactor design presented in **Figure 6** is adopted to calculate the capital cost of the sub-reactors. The reactor length is selected



to achieve a pressure drop of approximately 1 bar. The reactor is assumed to be constructed from high grade steel and provided with an inner insulation layer with a thickness of 470 mm that guarantees an outer wall temperature of around 60 °C. The steel shell thickness is calculated based on formulas from the ASME code section VIII-Division I ⁵⁰.

The reactor is equipped with elements for providing the necessary heat electrically and thermally conductive structures to ensure homogeneous distribution of the temperature inside the reactor. The costs considered for the reactor structure and the aforementioned conductive elements are reported in **Table 2**. The overall reactor cost is then increased by 50% to account for labor and installation, 14% for indirect costs, and 15% for owner and contingency costs, as considered by Riva et al. ²⁰. A mixture of conventional reforming Ni-based catalyst and CaO based sorbent spherical pellets, with a sorbent to catalyst volumetric ratio of 5, are assumed to fill the reactor. As they are subject to cyclic degradation, the catalyst and the sorbent are considered to be replaced annually to sustain the performance of the process. The cost of the function materials, catalyst and sorbent, are obtained from ²⁰.

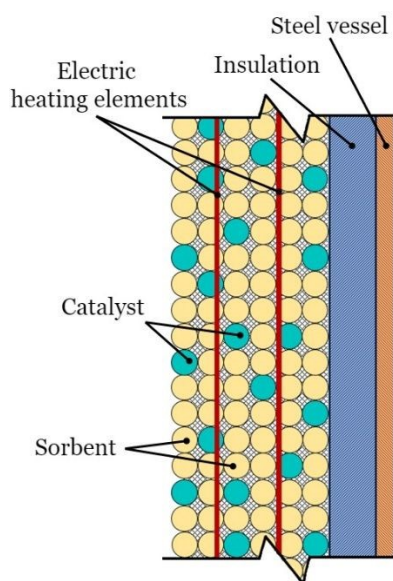


Figure 6 eSER reactor simplified design

Table 2 eSER reactor capital expenditure assumptions

Material	Specific Cost
Steel Vessel	9.6 €/kg
Insulation	18 €/kg



Electrical components	50	€/kW _{electric}
Conductive reactor internals	0.1	M€/m ³ _{reactor}

The different plant configurations are compared using the Levelized Cost of Hydrogen (LCOH), evaluating the cost of production of hydrogen over the lifetime of a hydrogen production plant, as a widely used metric in the industry. The plant is assumed to have a capacity factor of 86% resulting in 7500 equivalent operating hours. The fixed annual operating costs include annual maintenance cost of 1.5% of the total plant cost (TPC), and direct labor cost of 2.16M€/y (for 12 employees for each shift). The plant is projected to have a lifetime of 25 years. Besides, the consumables, obtained from ⁴⁸, and the variable costs used in this analysis are included in **Table 3**. The sensitivity of LCOH to natural gas prices, electricity prices, and CO₂ emission taxes is examined through a sensitivity analysis as reported in section 4.2. Additionally, the sensitivity of the LCOH to the Plant operating lifetime, Labor cost, and Capacity factor is reported in Section D of the supplementary Material.

Table 3 Assumed variable costs

Variable costs	Specific Cost
Natural gas	32.4 €/MWh _{LHV}
Electricity	60 €/MWh
Annual Catalyst replacement	50 €/kg
Annual Sorbent replacement	5 €/kg
CO ₂ transport and storage cost	25 €/t _{CO2 Captured}
CO ₂ emission tax	100 €/t _{CO2 Emitted}

4. Results and Discussion

This section outlines the findings of the study, which are divided into two subsections. Firstly, the technical analysis results are presented, followed by the economic analysis results.

4.1. Technical analysis results

Results of the simulations are summarized in **Table 4**. As a basis of comparison, the amount of feed NG is kept constant, calculated as the amount required for the production of 30000 Nm³/h of hydrogen in the base case. The temporal temperature and composition profiles downstream the



SER reactor during the reforming step, the stream properties tables and the TQ diagrams for heat recovery of the base case plant are reported in Section B of the supplementary material. The simulated eSER hydrogen production plant arrangements are compared with two hydrogen production plants utilizing amine based carbon capture units that are presented in the literature⁴⁸. The fired tubular reformer (FTR) plant represents the current commercial hydrogen production plants adopting conventional technologies. On the other hand, FTR Plus includes an advanced reforming plant, including an additional electrified reforming to improve methane conversion, a cooled low temperature water gas shift reactor to enhance the CO conversion, and increased CO₂ separation and H₂ recovery in the downstream syngas processing units. It is worth noting that the carbon capture units in both reference plants are located before the PSA units thus the carbon emitted from off gas combustion to balance the plant is released to the atmosphere.

Starting with a comparison between the base case and the reference benchmark plants, given the higher feed steam to carbon ratio of the eSER plant compared to the reference plants, a higher hydrogen production efficiency is computed. An exceptional energetic efficiency of 103.0% is calculated for the eSER plant representing 86.61% of the theoretical maximum hydrogen production on molar basis. On including the electric energy consumption, being a net electricity consumer, the eSER presents a total efficiency of 74.33% which is 1.91 percentage points lower than the conventional FTR plant and 0.62 points higher than the FTR Plus plant. It is worth mentioning that, on the contrary of the eSER plants, both the reference plants are net producers of electricity thus the calculated net efficiency includes the export of electric energy to the grid. Comparing the main environmental KPIs, the computed CCR of the base case eSER plant is 86.34% which is 7.46 percentage points higher than the conventional FTR reference plant but 4.18 percentage points lower than the FTR plus plant arrangement. Noteworthy, due to the higher hydrogen production simulated for the eSER plant, the specific emissions evaluated for the eSER plant is 0.90 kg_{CO2}/kg_{H2}, which is significantly lower than the 1.94 kg_{CO2}/kg_{H2} of the benchmark FTR plant and similar to 0.91 kg_{CO2}/kg_{H2} of the FTR Plus plant.



Table 4 Key performance indicators of the modeled plant arrangements.

		eSER Plants					Ref. Plants ⁴⁸	
		Base case	High Pressure	Vaccum Regen.	High S/C	eSER-eSMR - eSEWGS	FTR	FTR Plus
Reforming pressure	bar	10	30	10	10	30	32.7	32.7
Steam to carbon ratio	mol/mol	4.8	5.1	4.4	6	4.6	3.4	3.4
Regeneration pressure	bar	1	1	0.2	1	1	-	-
Regeneration temperature	°C	900	900	800	900	900	-	-
Natural gas thermal input	MW	86.63	86.63	86.63	86.63	86.63		
Hydrogen thermal output	MW	89.23	85.88	85.68	90.86	91.55		
Hydrogen output	Nm ³ /h	30000	28875	28806	30548	30780		
Hydrogen Production KPIs								
Total efficiency	%	74.33%	72.87%	73.51%	73.75%	73.12%	76.24%	73.71%
H ₂ production efficiency	MW _{H₂} /MW _{NG}	103.0%	99.1%	98.9%	104.9%	105.7%	74.6%	71.3%
Specific electricity consumption	kWh _{el} /kg _{H₂}	12.42	12.06	11.56	13.33	13.97	-0.61	-0.95
Environmental KPIs								
Specific CO ₂ Capture ratio	kg _{CO₂} /kg _{H₂}	5.68	5.84	5.70	5.83	6.19	7.16	8.60
Specific emission	kg _{CO₂} /kg _{H₂}	0.90	0.99	1.15	0.63	0.22	1.94	0.91
Specific emission	g _{CO₂} /MJ _{H₂}	7.49	8.27	9.60	5.24	1.83	16.16	7.58
Electricity consumption	kWh _{el} /kg _{CO₂ Cap.}	2.19	2.06	2.03	2.29	2.26	-0.09	-0.11
Carbon capture ratio	%	86.34%	85.48%	83.18%	90.27%	96.57%	78.88%	90.52%

The process block diagrams for the simulated plant arrangements are presented in Figure 2 for Base case, High pressure, Vacuum Regen.; Figure 4 for High S/C; and Figure 5 for eSER-eSMR-eSWGS.

Focusing on the effect of the different operational configurations of the eSER plants, on increasing the sorption enhanced reformer pressure from 10 to 30 bar, a reduction of the hydrogen production efficiency from 103.0% to 99.1% and of the total efficiency by 1.46 percentage points, from 74.33% to 72.87% compared to the base case are computed. This results in a decrease of the plant's hydrogen production from 30000 Nm³/h to 28875 Nm³/h for the same natural gas feed flow rate. This behavior can be explained by a drop of the methane conversion, which is evident by examining **Figure 7**, presenting the distribution of the uncaptured carbon leaving the process as off gas from the PSA unit. A significant increase in the uncaptured carbon is calculated, rising from 13.7% for the base case to 14.5% for the high-pressure case. The portion of the unconverted methane of the uncaptured carbon increased as well passing from 18% to 42% on operating the reformer at 30 bar. On the other hand, removing the need for a syngas compressor as the syngas is produced at the required pressure of the PSA unit leads to a reduction in the specific electricity consumption, which drops from 12.42 kWh/kgH₂ to 12.06 kWh/kgH₂ as reported in **Table 4**. The second configuration evaluates the performance of the eSER plant on operating the regeneration step of the process at sub atmospheric pressure, resulting in a reduction of the regeneration temperature. Compared to the base case, the vacuum regeneration case results in a drop in the hydrogen production efficiency from 103.0% to 98.9% and a reduction of the CCR from 86.3 to 83.2%. The lower regeneration temperature results in a lower initial bed temperature for the successive reforming step. Consequently, lower methane conversion is achieved leading to a drop in the hydrogen production and the CCR as explained in ³⁴. The significant reduction in the electricity consumption related to the reduced regeneration temperature helped in limiting the overall efficiency penalty of the vacuum regeneration case compared to the base case. Nevertheless, a reduction of the total efficiency by 0.79 percentage points is computed. As presented in **Figure 7**, the uncaptured carbon for this case shows a more uniform division between CH₄, CO, and CO₂ distributed as 35.2%, 37.3%, 27.5% of the total uncaptured carbon moles respectively.

Finally, the two advanced plant configurations aimed at achieving a CCR exceeding 90% are compared with the base case eSER plant, following the same approach employed for the different eSER configurations. Starting with the high steam to carbon case, a higher steam to carbon ratio (6.0 vs. 4.8 of the base case) is achieved by utilizing low temperature heat recovery for evaporating the additional quantity of steam required. Subsequently, the low-pressure steam (2 bar) is



pressurized to the selected reforming pressure of 10 bar using a steam compressor. Evaluating the key KPIs of this plant, it achieves a remarkable hydrogen production efficiency of 104.9%. However, compared to the base case, the electric demand of the steam compressor increases the specific electric consumption from 12.42 to 13.33 kWh/kg_{H2}, resulting in a loss of 0.58 percentage points in the overall plant efficiency. The high steam to carbon ratio results in a higher extent of the SR and WGS reactions resulting in a higher concentration of the CO₂ in the PSA off gas as shown in **Figure 7**. The final simulated plant is designed to achieve high methane conversion at high pressure, facilitated by the addition of a subsequent eSMR reactor operating at 950°C followed by a high temperature eSEWGS to maximize hydrogen production and carbon capture. Comparing the KPIs of the eSER-eSMR-eSEWGS plant with the base case eSER plant, a significant increase in hydrogen production efficiency from 103.0% to 105.7% is observed representing the highest hydrogen production efficiency of all the simulated plants. Nevertheless, the overall efficiency dropped by 1.21 percentage points as a result of the increase in electricity consumption from 12.42 to 13.97 kWh/kg_{H2}. Notably, the eSER-eSMR-eSEWGS arrangement shows a remarkably high carbon capture ratio reaching 96.57%.

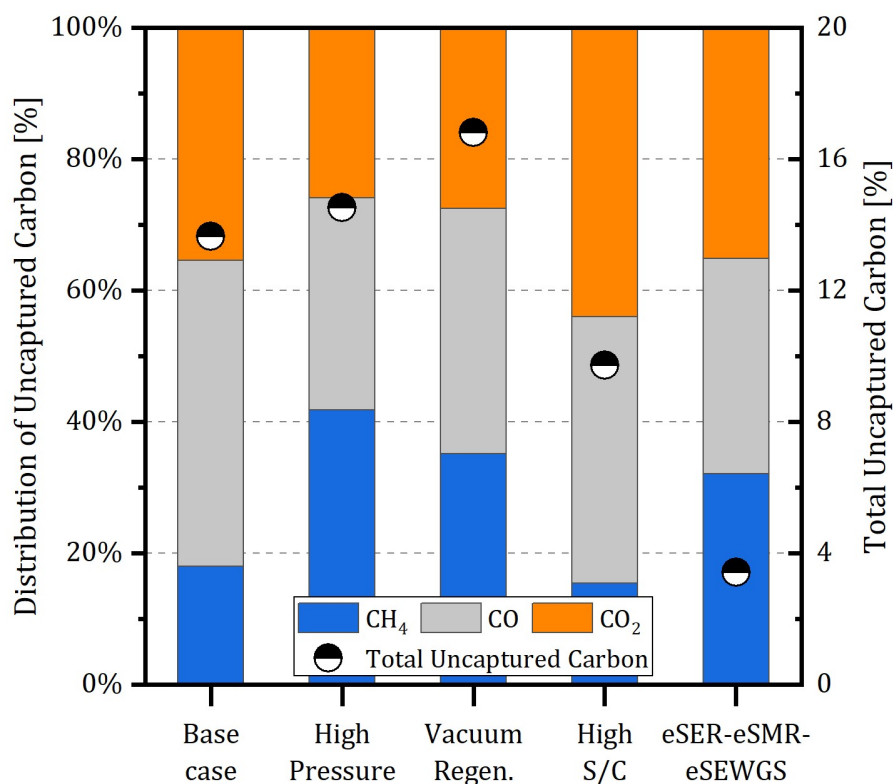


Figure 7 PSA off-gas C-containing species molar percent



Focusing on the electricity consumption, **Figure 8** illustrates the contribution of the different parts of the plant on the specific electricity consumption for the simulated eSER arrangements. The energy demand of the regeneration step of the process includes the sensible heat, to heat up the saturated sorbent to the regeneration temperature, and the enthalpy required for CaCO_3 decomposition. As evident in the figure, more than 40% of the total consumed energy is attributed to CaCO_3 decomposition for all the simulated plants. The next significant contribution is related to heating the reactor up to the necessary sorbent regeneration temperature. With the exception of the eSER-eSMR-eSEWGS plant, these two contributions collectively represent more than 85% of the specific electricity consumption for the simulated plants. Notably, the vacuum regeneration case, where the sorbent regeneration takes place under sub atmospheric conditions hence at lower temperature, presents the lowest specific electricity consumption. In this case, compared to the base case, the increase in power consumption for CO_2 compression is less than the reduction in the energy required to heat the reactor leading to a total drop of electricity consumption from 12.42 to 11.56 kWh/kgH_2 .

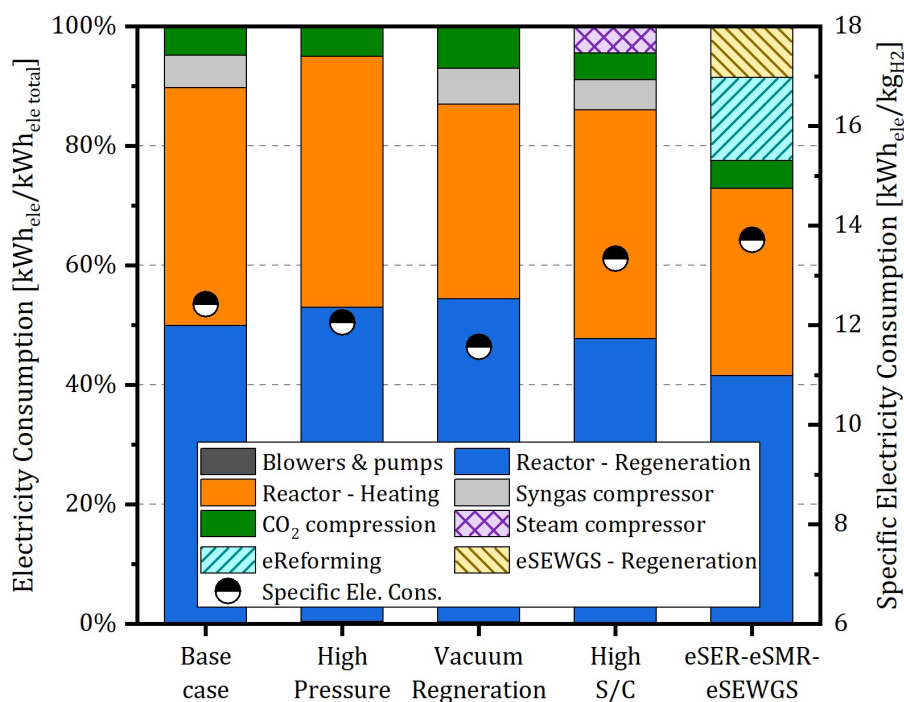


Figure 8 Specific electricity consumption breakdown

Being the eSER a technology with a high electricity consumption which is evaluated for fossil-based feeds, assessing the environmental performance of the eSER plants requires consideration of both



direct emissions from the combustion of the PSA off gas and indirect emissions related to the carbon intensity of the consumed electricity and the methane leakage from the natural gas supply chain. As defined in Eq. 4, Equivalent CO₂ emissions ($E_{CO_2, eq}$) is used for such analysis. The analysis considers an impact of 82.5 kgCO_{2 eq}/kgCH₄ over a 20 years time-horizon (GWP20) and 29.8 kgCO_{2 eq}/kgCH₄ over 100 years (GWP100) ⁴. Comparing the calculated $E_{CO_2, eq}$ of the different eSER arrangements, as presented in **Figure 9**, the key role of the carbon intensity of the consumed electricity along with the methane leakage from the natural gas supply chain is evident. In fact, upon considering electricity mix with carbon intensity of 50 kgCO₂/MWh_{el}, all the simulated plant arrangements resulted in $E_{CO_2, eq}$ higher than 1 kgCO_{2eq}/kgH₂, the threshold for Ultralow-carbon hydrogen defined by World Business Council for Sustainable Development. However, the calculated $E_{CO_2, eq}$ for all the simulated plants remains below the threshold for the Low-carbon Hydrogen of 3 kgCO_{2eq}/kgH₂ even when considering 0.5% CH₄ leakage, representative of a low carbon intensity natural gas supply chain ⁵¹. Without methane leakage the eSER-eSMR-eSEWGS presents the lowest $E_{CO_2, eq}$ of 1.09 kgCO_{2eq}/kgH₂ rising up to 2.10 on considering 0.5% CH₄ leakage. For the sake of comparison, the calculated $E_{CO_2, eq}$ of water electrolysis, with 65% efficiency (LHV-basis), using the same electricity mix is 2.56 kgCO_{2eq}/kgH₂. Following the eSER-eSMR-eSEWGS case, the calculated $E_{CO_2, eq}$ of the high steam to carbon case is 1.30 kgCO_{2eq}/kgH₂ without CH₄ leakage and 2.30 kgCO_{2eq}/kgH₂ with 0.5% CH₄ leakage, representing an improvement compared to the base case of 0.22 and 0.24 kgCO_{2eq}/kgH₂ respectively. A breakdown of the contribution of direct and indirect emissions on the $E_{CO_2, eq}$ for the simulated eSER plants compared with the benchmark hydrogen production via electrolysis is presented in **Figure 9**.



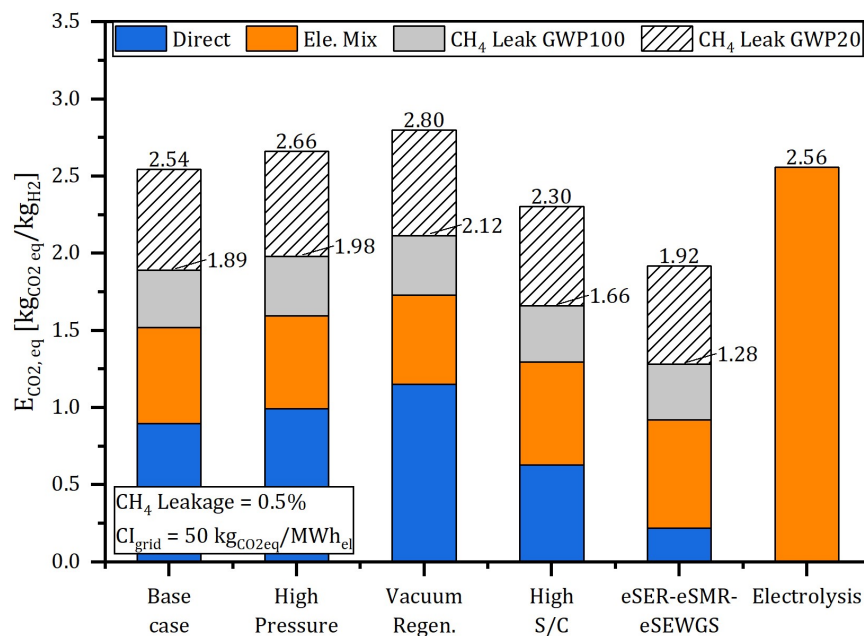


Figure 9 $E_{CO_2,eq}$ breakdown. CH₄ leakage

A sensitivity analysis is performed to evaluate the impact of the methane leakage and the carbon intensity of the consumed electricity on the $E_{CO_2,eq}$. **Figure 10** shows the effect of the carbon intensity of the electricity consumed (left) and the methane leakage (right) on the $E_{CO_2,eq}$ calculated for the base case (black lines), high steam to carbon case (red lines), and the eSER-eSMR-eSEWGS case (green lines). The analysis examines the impact of the methane leakage over 20 years (GWP20), and 100 years (GWP100) represented by the solid and the dashed lines respectively.

Starting with the effect of the electricity carbon intensity, assuming a constant value for the CH₄ leakage of 0.5% and considering GWP20, the calculated $E_{CO_2,eq}$ for the base case ranges from 1.92 kg_{CO₂eq}/kg_{H₂} when using completely carbon-free electricity to 5.65 kg_{CO₂eq}/kg_{H₂} with a grid carbon intensity of 300 kg_{CO₂}/MWh_{el}. These values reduce to 1.27 and 4.99 kg_{CO₂eq}/kg_{H₂} respectively on considering GWP100. Relative to the water electrolysis technology, represented by the blue line in the figure, the computed $E_{CO_2,eq}$ of water electrolysis is 0 kg_{CO₂eq}/kg_{H₂} for carbon free electricity and rises dramatically, due to the high consumption of electricity, with the grid carbon intensity exceeding 15.3 kg_{CO₂eq}/kg_{H₂} on considering a grid carbon intensity of 300 kg_{CO₂}/MWh_{el}. Noteworthy, the average carbon intensity of electricity generation in the EU is 244 kg_{CO₂}/MWh_{el}.⁵²

Regarding the eSER cases with the highest CCR, considering GWP20, the calculated $E_{CO_2,eq}$ high steam to carbon case is 1.64 kg_{CO₂eq}/kg_{H₂} with carbon free electricity rising to 5.64 kg_{CO₂eq}/kg_{H₂}



considering a grid carbon intensity of $300 \text{ kg}_{\text{CO}_2}/\text{MWh}_{\text{el}}$. The eSER-eSMR-eSEWGS case shows the best performance of all the examined cases with an $E_{\text{CO}_2, \text{eq}}$ of 1.22 and 5.41 considering the fully decarbonized grid and a typical grid with a carbon intensity of $300 \text{ kg}_{\text{CO}_2}/\text{MWh}_{\text{el}}$ respectively.

Looking at the effect of the CH_4 leakage on the environmental performance of the eSER plants, a significant impact is evident. With no methane leakage, considering grid carbon intensity of $50 \text{ kg}_{\text{CO}_2}/\text{MWh}_{\text{el}}$, the $E_{\text{CO}_2, \text{eq}}$ of the base case, high steam to carbon case, and eSER-eSMR-eSEWGS case are 1.52, 1.30, and $0.92 \text{ kg}_{\text{CO}_2\text{eq}}/\text{kg}_{\text{H}_2}$ respectively. However, considering GWP20, a 1% increase in the methane leakage results in an important increase in the $E_{\text{CO}_2, \text{eq}}$ reaching 3.57, 3.31, and $2.92 \text{ kg}_{\text{CO}_2\text{eq}}/\text{kg}_{\text{H}_2}$ for the three examined plants respectively. A comparison between the estimated Equivalent CO_2 emissions for the different eSER configurations and the reference FTR plants is reported in Section C of the Supplementary Materials of this work.

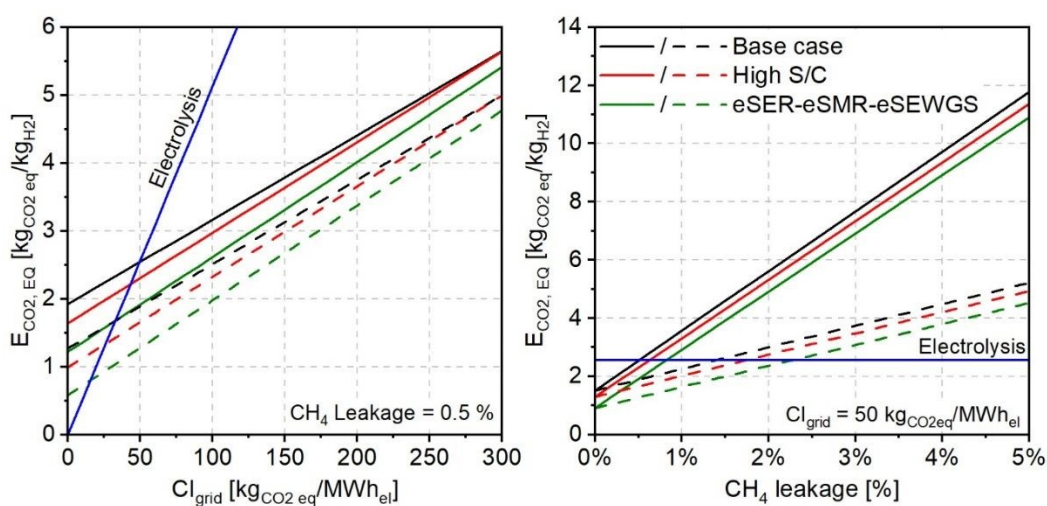


Figure 10 $E_{\text{CO}_2, \text{eq}}$ for the base case, high steam to carbon, and eSER-eSMR-eSEWGS plants as a function of CI_{grid} (Left) and CH_4 leakage (Right). Solid lines refer to GWP20 and dashed lines to GWP100.

4.2. Economic analysis results

Following the “bottom-up” method as explained in section 3 of this work, the calculated capital expenditure (CAPEX) breakdown is reported in **Table 5**. The calculated total CAPEX of the base case is 82.81 M€ of which 43.3% are related to the cost of the eSER reactors, and 32.8% associated to the steam generation and heat recovery section of the plant (Heat exchangers). The estimated cost of the syngas compressor and CO_2 compressor are 6.39 M€, and 5.98 M€ representing 7.7%,



and 7.2% of the total plant CAPEX. Designing the process for higher operating pressure of the reformer (High pressure case), results in eliminating the cost of the syngas compressor. However, the increase in the operating pressure of the reformer leads to significantly increase the cost of the reactor vessels by 9.39 M€ resulting in a higher total CAPEX of the high-pressure case compared to the base case.

The calculated CAPEX breakdown for the Vacuum regeneration case shows a significant reduction of the heat exchangers cost compared to the base case, given that lower regeneration temperature is used resulting in a lower need of heat recovery. Instead, as the regeneration step of the process operates in sub atmospheric pressures, the computed CO₂ compressor CAPEX is higher. Overall, the estimated total CAPEX of the vacuum regeneration case is the lowest among all the examined plant arrangements.

The two plants with the added constraint of having a CCR higher than 90% show a higher CAPEX compared to the base case. The estimated total CAPEX of high steam to carbon case and the eSER-eSMR-eSEWGS cases are 83.48, and 94.01 M€ respectively.

Table 5 Capital expenditure breakdown for the modeled eSER plant configurations

		Base case	High Pressure	Vacuum Regeneration	High S/C	eSER-eSMR-eSEWGS
Blowers and pumps	M€	0.39	0.46	0.42	0.35	0.50
Desulfurization unit	M€	0.35	0.34	0.38	0.31	0.39
Heat exchangers	M€	27.17	25.64	24.40	27.44	23.35
eSER reactors	M€	35.83	45.22	34.78	35.74	45.86
Syngas compressor	M€	6.39	-	6.77	5.70	-
CO ₂ compression	M€	5.98	5.77	7.77	5.46	7.01
PSA	M€	6.69	6.16	7.26	5.65	7.79
Steam compressor	M€	-	-	-	2.81	-
eReformer	M€	-	-	-	-	2.15
eSEWGS reactors	M€	-	-	-	-	6.97
Total	M€	82.81	83.59	81.78	83.48	94.01



As presented in **Figure 11**, the levelized cost of hydrogen is used to compare the different simulated configurations. The computed LCOH for the base case is 2.50 €/kg_{H2}, which is comparable to the value of 2.27 €/kg_{H2} obtained for the FTR-Plus plant from the literature⁴⁸. For all the simulated cases, the cost of natural gas represents the highest share of the cost of hydrogen followed by the cost of electricity. Operating the eSER process at high pressure or using the vacuum regeneration approach result in a higher LCOH as a result of the combined effect of the reduced hydrogen production efficiency and the carbon capture ratio, resulting in higher CO₂ emission tax. A detailed breakdown of the estimated annual costs, used for the calculation of the LCOH, for all the simulated cases is provided in **Table 6**. It is worth noting that the CAPEX has a minor effect on the LCOH where even if the calculated CAPEX for the eSER-eSMR-eSEWGS case is 12.7% higher than the base case, the LCOH increases by less than 1% only.

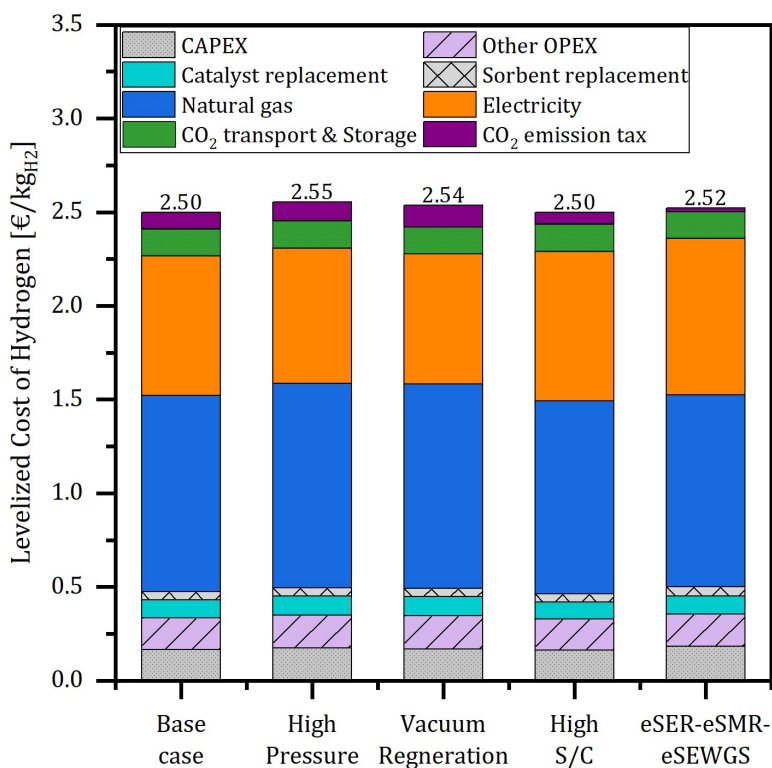


Figure 11 Levelized cost of hydrogen for the eSER modeled plant arrangements



Table 6 Annual costs distribution for the different modeled plant arrangements

Annual Cost		Base case	High Pressure	Vacuum Regeneration	High S/C	eSER-eSMR-eSEWGS
Capital expenditure	M€/y	3.31	3.34	3.27	3.34	3.76
Natural gas	M€/y	21.05	21.05	21.05	21.05	21.05
Catalyst replacement	M€/y	1.95	1.97	1.97	1.82	1.97
Sorbent replacement	M€/y	0.86	0.86	0.86	0.86	1.03
Electricity	M€/y	14.95	13.98	13.37	16.36	17.27
CO ₂ transport & Storage	M€/y	2.85	2.82	2.75	2.98	2.90
CO ₂ emission tax	M€/y	1.80	1.92	2.22	1.29	0.41
Other OPEX	M€/y	3.40	3.41	3.39	3.41	3.57
Levelized cost of H ₂	€/kg _{H2}	2.50	2.55	2.54	2.50	2.52

Figure 12 Presents a sensitivity analysis performed on the LCOH for three of the simulated cases: the base case, the high steam to carbon case, and the eSER-eSMR-eSEWGS case. The natural gas price (Panel A) shows an almost equivalent effect on the three cases with a minor advantage for the high steam to carbon case as it has the highest H₂ production efficiency. The electricity price (Panel B) presents a strong effect as well, where, in the presence of cheap electricity, high steam to carbon case becomes the most competitive case. The LCOH is evidently less sensitive to the CO₂ tax, where a slight increase in the LCOH for all the evaluated cases is observed with the increase of a carbon tax. The favorable carbon capture performance of the high steam to carbon and eSER-eSMR-eSEWGS cases makes them more competitive plant arrangements in the presence of a high carbon tax. The base case presents the most competitive configuration in the absence of a carbon tax but is surpassed with a tax higher than 100 €/ton_{CO2} by the high steam to carbon case. When the carbon tax exceeds 150 €/ton_{CO2} the eSER-eSMR-eSEWGS case becomes the most economic option. Additionally, as reported in panel D of **Figure 12**, the number of reactors is considered as a sensitivity parameter as well; where in all the aforementioned simulations, 12 sub-reactors are considered as explained in section 3.1. However, a case where additional reactors may be needed to manage the depressurization/purge/re-pressurization stages hence the sensitivity of the LCOH to this parameter is evaluated. Evidently, the LCOH is less sensitive to the number of sub-reactors,



as this number primarily impacts the CAPEX, which accounts for approximately 7% of the LCOH for all simulated cases.

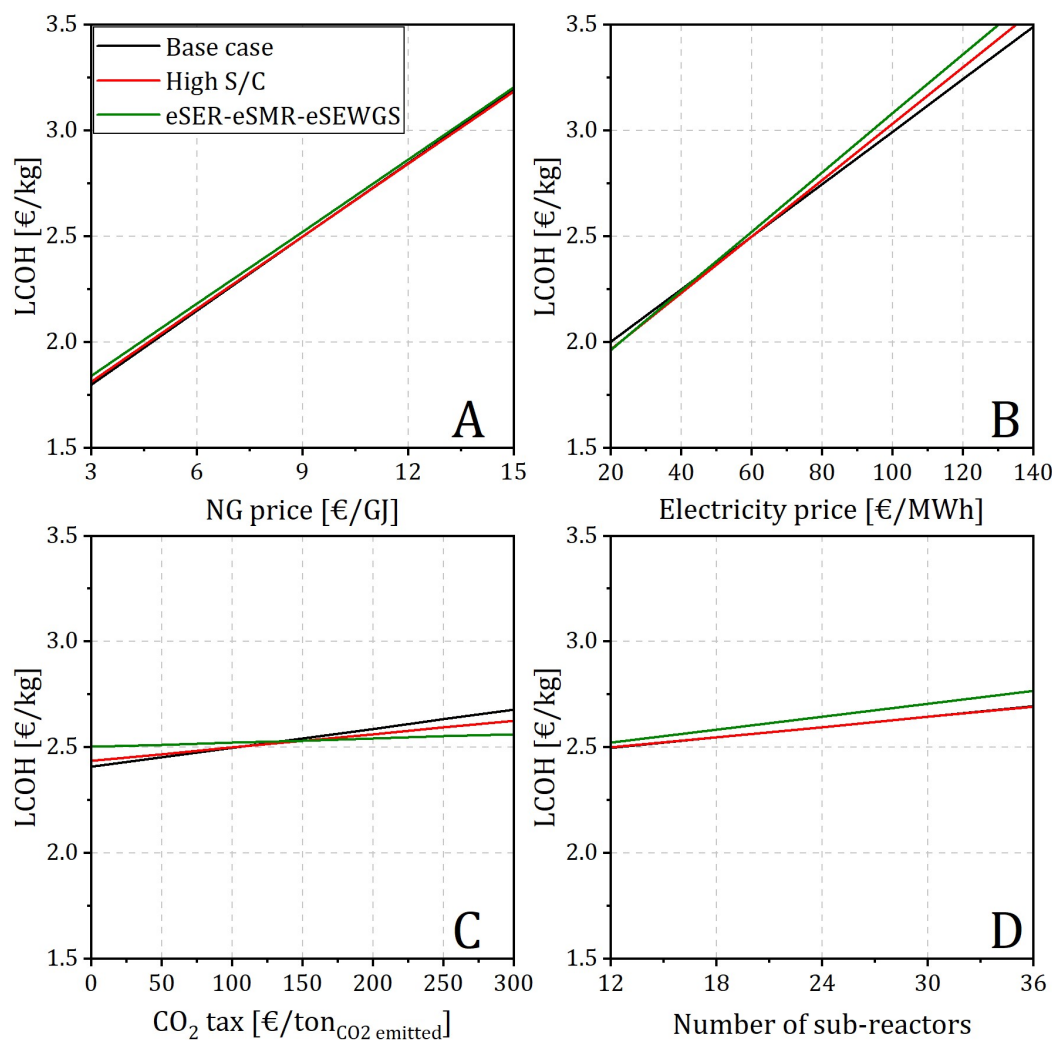


Figure 12 Effect of A) natural gas price, B) electricity price, C) CO₂ tax, and D) number of reactors, on the levelized cost of hydrogen for the base case, high S/C, and eSER-eSMR-eSEWGS arrangements

5. Conclusions

This study assesses the technical and economic performance of the novel electrified sorption enhanced reforming (eSER) process. The process leverages reactor electrification concept for covering the thermal demand of the endothermic sorbent regeneration step in sorption enhanced reforming. Electrified regeneration of SER packed bed allows to overcome the limitations of



conventional SER systems regenerated via heat transfer surfaces or additional chemical looping cycles (i.e. the Ca-Cu), significantly improving the technical feasibility of the process. In this work, natural gas-based hydrogen production plants with H₂ production capacity of 30000 Nm³/h are considered. In the core of the process, electrified reactors are assumed as a bundle of sub-reactors that share the same set of valves where each of the sub-reactors is modeled using a 1-D dynamic heterogeneous model of an adiabatic fixed bed reactor. Five different cases are simulated with different operating conditions or plant arrangements. These simulated cases are compared with benchmark technology existing in the literature. The study shows that:

- eSER achieves natural gas to H₂ efficiency on LHV basis exceeding 100% and specific electric consumption of 12-14 kWh/kg_{H₂}.
- Due to the competition between CH₄ reforming (favored by high temperature and low pressure) and CO₂ sorption by carbonation reaction (favored by low temperature and high pressure), it is challenging for SER processes to achieve carbon capture ration (CCR) higher than 90%. In the base case (P_{SER} 10 bar, P_{REG} 1 bar), CCR of 86.3% was achieved. Increasing SER pressure and decreasing regeneration pressure and temperature led to the reduction of the CCR.
- To achieve >90% CCR, two options have been explored: 1) very high S/C (=6), where steam is partly supplied by LP evaporator and steam compressor, which led to CCR 90.3%; 2) three-reactor process, where the eSER reactor is followed by an electrified steam methane reformer (eSMR) and an electrified CaO-based sorption-enhanced water gas shift reactor (eSEWGS), achieving CCR=96.6% thanks to the decoupling between SMR and carbonation reactions after the primary eSER, where the bulk of the two reactions is carried out.
- With electricity carbon intensity of 50 kg/MWh and CH₄ leakage rate from the natural gas supply chain of 0.5%, total 100y carbon footprint of eSER systems resulted between 1.9 kg_{CO₂}/kg_{H₂} (high CCR case) and 2.5 kg_{CO₂}/kg_{H₂} (base case), comparable to the carbon footprint of electrolytic hydrogen (2.6 kg_{CO₂}/kg_{H₂}) with 65% electrolysis efficiency.
- With baseline assumptions (NG cost 9 €/GJ, electricity cost 60 €/MWh), levelized cost of hydrogen between 2.5 and 2.6 €/kg has been estimated, most of the cost is associated to natural gas cost (42-44%) and to electricity cost (28-32%).



Acknowledgements

This work has received fundings from M.U.R. Progetti di Ricerca di Rilevante Interesse Nazionale (PRIN) Bando 2020 under the project (2020N38E75- “PLUG-IN”).

Conflicts of interest

There are no conflicts of interest to declare.

References

- 1 G. Natrella, A. Borgogna, A. Salladini and G. Iaquaniello, *Clean. Eng. Technol.*, 2021, **5**, 100280.
- 2 IEA, Global Hydrogen Review 2023, <https://www.iea.org/reports/global-hydrogen-review-2023>, (accessed 6 December 2023).
- 3 S. T. Wismann, J. S. Engbæk, S. B. Vendelbo, W. L. Eriksen, C. Frandsen, P. M. Mortensen and I. Chorkendorff, *Chem. Eng. J.*, , DOI:10.1016/j.cej.2021.131509.
- 4 M. C. Romano, C. Antonini, A. Bardow, V. Bertsch, N. P. Brandon, J. Brouwer, S. Campanari, L. Crema, P. E. Dodds, S. Gardarsdottir, M. Gazzani, G. Jan Kramer, P. D. Lund, N. Mac Dowell, E. Martelli, L. Mastropasqua, R. C. McKenna, J. G. M. S. Monteiro, N. Paltrinieri, B. G. Pollet, J. G. Reed, T. J. Schmidt, J. Vente and D. Wiley, *Energy Sci. Eng.*, 2022, **10**, 1944–1954.
- 5 A. M. Adris, B. B. Pruden, C. J. Lim and J. R. Grace, *Can. J. Chem. Eng.*, 1996, **74**, 177–186.
- 6 Y. Yan, D. Thanganadar, P. T. Clough, S. Mukherjee, K. Patchigolla, V. Manovic and E. J. Anthony, *Energy Convers. Manag.*, 2020, **222**, 113144.
- 7 A. R. Brun-Tsekhovoi, S. S. Kurdyumov, Y. R. Katsobashvili and N. V. Sidorova, *Chem. Technol. Fuels Oils*, 1976, **12**, 97–101.
- 8 B. Balasubramanian, A. L. Ortiz, S. Kaytakoglu and D. P. Harrison, *Chem. Eng. Sci.*, 1999, **54**, 3543–3552.
- 9 C. Han and D. P. Harrison, *Chem. Eng. Sci.*, 1994, **49**, 5875–5883.
- 10 K. Johnsen, J. R. Grace, S. S. E. H. Elnashaie, L. Kolbeinsen and D. Eriksen, *Ind. Eng. Chem. Res.*, 2006, **45**, 4133–4144.
- 11 S. Masoudi Soltani, A. Lahiri, H. Bahzad, P. Clough, M. Gorbounov and Y. Yan, *Carbon Capture Sci. Technol.*, 2021, **1**, 100003.
- 12 J. Mays, *One Step Hydrogen Generation Through Sorption Enhanced Reforming*, Golden, CO (United States), 2017.
- 13 I. Martínez, M. C. Romano, P. Chiesa, G. Grasa and R. Murillo, *Int. J. Hydrogen Energy*, 2013, **38**, 15180–15199.



- 14 L. Zhu and J. Fan, *Int. J. Energy Res.*, 2015, **39**, 356–369.
- 15 S. Alam, J. P. Kumar, K. Y. Rani and C. Sumana, *J. Clean. Prod.*, 2017, **162**, 687–701.
- 16 A. Phuluanglue, W. Khaodee and S. Assabumrungrat, *Comput. Chem. Eng.*, 2017, **105**, 237–245.
- 17 M. C. Romano, E. N. Cassotti, P. Chiesa, J. Meyer and J. Mastin, *Energy Procedia*, 2011, **4**, 1125–1132.
- 18 US8506915B2, 2009.
- 19 I. Martínez, J. R. Fernández, M. Martini, F. Gallucci, M. van Sint Annaland, M. C. Romano and J. C. Abanades, *Int. J. Greenh. Gas Control*, 2019, **85**, 71–85.
- 20 L. Riva, I. Martínez, M. Martini, F. Gallucci, M. van Sint Annaland and M. C. Romano, *Int. J. Hydrogen Energy*, 2018, **43**, 15720–15738.
- 21 M. C. Iliuta, in *Advances in Chemical Engineering*, Academic Press Inc., 2017, vol. 51, pp. 97–205.
- 22 A. N. Antzaras and A. A. Lemonidou, *Renew. Sustain. Energy Rev.*, 2022, **155**, 111917.
- 23 E. Tronconi, G. Groppi and C. G. Visconti, *Curr. Opin. Chem. Eng.*, 2014, **5**, 55–67.
- 24 C. G. Visconti, G. Groppi and E. Tronconi, *Catal. Today*, 2016, **273**, 178–186.
- 25 M. Ambrosetti, *Chem. Eng. Process. - Process Intensif.*, 2022, **182**, 109187.
- 26 M. G. Vinum, M. R. Almind, J. S. Engbæk, S. B. Vendelbo, M. F. Hansen, C. Frandsen, J. Bendix and P. M. Mortensen, *Angew. Chemie - Int. Ed.*, 2018, **57**, 10569–10573.
- 27 M. R. Almind, S. B. Vendelbo, M. F. Hansen, M. G. Vinum, C. Frandsen, P. M. Mortensen and J. S. Engbæk, *Catal. Today*, 2020, **342**, 13–20.
- 28 V. Poletto Dotsenko, M. Bellusci, A. Masi, D. Pietrogiacomini and F. Varsano, *Catal. Today*, 2023, **418**, 114049.
- 29 E. Meloni, M. Martino, A. Ricca and V. Palma, *Int. J. Hydrogen Energy*, 2021, **46**, 13729–13747.
- 30 S. T. Wismann, J. S. Engbæk, S. B. Vendelbo, F. B. Bendixen, W. L. Eriksen, K. Aasberg-Petersen, C. Frandsen, I. Chorkendorff and P. M. Mortensen, *Science (80-.)*, 2019, **364**, 756–759.
- 31 L. Zheng, M. Ambrosetti, D. Marangoni, A. Beretta, G. Groppi and E. Tronconi, *AIChE J.*, , DOI:10.1002/aic.17620.
- 32 L. Zheng, M. Ambrosetti, F. Zaio, A. Beretta, G. Groppi and E. Tronconi, *Int. J. Hydrogen Energy*, 2023, **48**, 14681–14696.
- 33 WO2023062591A1, .
- 34 A. Mostafa, I. Rapone, A. Bosetti, M. C. Romano, A. Beretta and G. Groppi, *Int. J. Hydrogen Energy*, 2023, **48**, 26475–26491.



- 35 V. Spallina, F. Gallucci, M. C. Romano and M. Van Sint Annaland, *Chem. Eng. J.*, 2016, **294**, 478–494.
- 36 I. Martínez, D. Armaroli, M. Gazzani and M. C. Romano, *Ind. Eng. Chem. Res.*, 2017, **56**, 2526–2539.
- 37 V. Spallina, B. Marinello, F. Gallucci, M. C. Romano and M. Van Sint Annaland, *Fuel Process. Technol.*, 2017, **156**, 156–170.
- 38 H. P. Hamers, M. C. Romano, V. Spallina, P. Chiesa, F. Gallucci and M. Van Sint Annaland, *Appl. Energy*, 2015, **157**, 422–432.
- 39 S. Cloete, A. Giuffrida, M. Romano, P. Chiesa, M. Pishahang and Y. Larring, *Fuel*, 2018, **220**, 725–743.
- 40 S. Cloete, M. C. Romano, P. Chiesa, G. Lozza and S. Amini, *Int. J. Greenh. Gas Control*, 2015, **42**, 340–356.
- 41 J. R. Fernández, J. C. Abanades, R. Murillo and G. Grasa, *Int. J. Greenh. Gas Control*, 2012, **6**, 126–141.
- 42 I. Martínez, R. Murillo, G. Grasa, J. R. Fernández and J. C. Abanades, *AIChE J.*, 2013, **59**, 2780–2794.
- 43 A. Mostafa, I. Rapone, A. Bosetti, M. C. Romano, A. Beretta and G. Groppi, *Ind. Eng. Chem. Res.*, 2023, **62**, 15884–15896.
- 44 E. H. Baker, *J. Chem. Soc.*, 1962, 464–470.
- 45 R. Balzarotti, M. Ambrosetti, A. Beretta, G. Groppi and E. Tronconi, *Chem. Eng. J.*, 2020, **391**, 123494.
- 46 L. Zheng, M. Ambrosetti, A. Beretta, G. Groppi and E. Tronconi, *Chem. Eng. J.*, 2023, **466**, 143154.
- 47 X. Wang, N. Wang and L. Wang, *Int. J. Hydrogen Energy*, 2011, **36**, 466–472.
- 48 A. de Cataldo, M. Astolfi, P. Chiesa, S. Campanari and M. C. Romano, *Int. J. Hydrogen Energy*, 2023, **49**, 978–993.
- 49 R. Turton, R. C. Bailie, W. B. Whiting, J. A. Shaeiwitz and D. Bhattacharyya, *Analysis, Synthesis, and Design of Chemical Processes*, 2001, vol. 40.
- 50 S. C. Roberts, in *Online Companion Guide to the ASME Boiler & Pressure Vessel Codes*, ASME Press, 2020, p. 114.
- 51 J. Pettersen, R. Steeneveldt, D. Grainger, T. Scott, L. M. Holst and E. S. Hamborg, *Energy Sci. Eng.*, 2022, **10**, 3220–3236.
- 52 M. Wiatros-Motyka, N. Fulghum, D. Jones, K. Altieri, R. Black, H. Broadbent, C. Bruce-Lockhart, M. Ewen, P. MacDonald, K. Rangelova, S. Brown, L. Copsy, R. Dizon, S. Hawkins, L. Heberer, S. Hong, R. Hutt, U. Lee, A. Lolla, J. Murdoch, J. Robinson, N. Rodrigues, C. Rosslowe and O. Zaimoglu, *Global Electricity Review 2024*, 2024.



Open Access Article. Published on 11 mars 2025. Downloaded on 2025-03-15 02:51:52.
This article is licensed under a Creative Commons Attribution 3.0 Unported Licence.



The cost function parameters and scaling function parameters used for the economic analysis, as well as the stream properties used for the technical analysis are reported in the supplementary material of this work. Other data are available upon request.

